Classification: Biological Sciences (Developmental Biology)

Intronic delay is essential for oscillatory expression in the segmentation clock

Yoshiki Takashima[1-3], Toshiyuki Ohtsuka[1,2], Aitor González[1,2], Hitoshi Miyachi[1], and Ryoichiro Kageyama[1,2]*

[1]Institute for Virus Research, Kyoto University, Shogoin-Kawahara, Sakyo-ku, Kyoto 606-8507, Japan; [2]Japan Science and Technology Agency, CREST, Shogoin-Kawahara, Sakyo-ku, Kyoto 606-8507, Japan; [3]Kyoto University Graduate School of Biostudies, Kyoto 606-8502

*Corresponding author: Ryoichiro Kageyama
Institute for Virus Research
Kyoto University
Shogoin-Kawahara, Sakyo-ku
Kyoto 606-8507
Japan
Tel: 81-75-751-4011
Fax: 81-75-751-4807
E-mail: rkageyam@virus.kyoto-u.ac.jp

Running title: Intronic delay in oscillatory expression

Keywords: *Hes7*; intronic delay; negative feedback; oscillation; segmentation clock; somitogenesis

Abstract

Proper timing of gene expression is essential for many biological events, but the molecular mechanisms that control timing remain largely unclear. It has been suggested that introns contribute to the timing mechanisms of gene expression, but this hypothesis has not been tested with natural genes. One of the best systems for examining the significance of introns is the oscillator network in the somite segmentation clock, because mathematical modeling predicted that oscillating expression depends on negative feedback with a delayed timing. The basic helix-loop-helix repressor gene *Hes7* is cyclically expressed in the presomitic mesoderm (PSM) and regulates the somite segmentation. Here, we found that introns lead to a ~19-min delay in the *Hes7* gene expression, and mathematical modeling suggested that without such a delay, Hes7 oscillations would be abolished. To test this prediction, we generated mice carrying the *Hes7* locus whose introns were removed. In these mice, Hes7 expression did not oscillate but occurred steadily, leading to severe segmentation defects. These results indicate that introns are indeed required for Hes7 oscillations, and point to the significance of intronic delays in dynamic gene expression.

¥body

Introduction

Proper timing of activation and repression of gene expression is essential for many biological events, but the molecular mechanisms that control timing remain largely unclear. It has been suggested that introns contribute to the timing mechanisms of gene expression (1-3), but this hypothesis has not been tested with natural genes. One of the best systems for examining the significance of introns is the oscillator network in the somite segmentation clock (4-9).

During somite segmentation of mouse embryos, the basic helix-loop-helix repressor gene *Hes7* is cyclically expressed with a period of about 2 hours in the presomitic mesoderm (PSM) (10). Hes7 expression domain is propagated from the posterior to the anterior PSM, and each cycle leads to formation of a bilateral pair of somites (10). Both loss of expression and persistent expression of *Hes7* lead to somite

fusion, suggesting that oscillatory expression is required for periodic somite segmentation (10,11). This oscillatory expression is regulated by negative feedback similar to the regulation of Hes1 in fibroblasts (12): Hes7 protein represses transcription from the *Hes7* promoter, and this repression down-regulates both *Hes7* mRNA and Hes7 protein levels. This results in relief from the negative feedback and allows the next round of expression (13). Transcription of the *Hes7* gene and accumulation of Hes7 protein occur in a mutually exclusive manner, and therefore these two events proceed alternately every two hours, indicating that Hes7 protein accumulation is substantially delayed relative to *Hes7* gene transcription (Fig. 1A) (13). This negative feedback-mediated oscillatory expression has been mathematically simulated by differential equations (14-17). These models predict that the delay from transcription to protein expression and then to negative autoregulation must be sufficiently long for sustained oscillations, and that short delays would abolish oscillations. However, this prediction has not been experimentally tested yet.

In order to determine the significance of introns in the timing of gene expression, we focused on the *Hes7* gene in the mouse segmentation clock. We first found that the *Hes7* promoter-driven reporter without any introns led to expression about 19 min earlier than the reporter with full introns, indicating that introns lead to about a 19-min delay in Hes7 expression. According to our previous mathematical model (17), if the delay is 19 min shorter, the oscillatory expression of Hes7 would be abolished, although a different model predicted sustained oscillations without delays (18). To determine whether intronic delays are required for sustained oscillations of Hes7 expression, we generated mice carrying the *Hes7* locus whose introns were removed. We found that Hes7 oscillations were abolished in these mutant mice and that somites were not properly segmented. These data indicate that intronic delays are essential for sustained Hes7 oscillations and periodic somite segmentation.

Results and Discussion

Both intron-plus and intron-minus *Hes7* reporters display oscillatory expression

To assess the significance of introns in the timing of gene expression, we first generated two *Hes7* promoter-driven reporters: one carried no introns (pH7-UbLuc-In(–), 3,070-

bp transcript, Fig. 1B), while the other carried all *Hes7* gene introns (pH7-UbLuc-In(+), 4,913-bp transcript, Fig. 1B). This promoter fragment was previously shown to contain regulatory elements required for normal *Hes7* expression (11). Because the half-life of Hes7 protein is about 20 min (17), that of a reporter should be 20 min or shorter. Otherwise, a reporter protein would be accumulated after several cycles. We previously showed that a ubiquitinated luciferase (Ub-luc) can be successfully used as a reporter for *Hes1*, which also displays oscillatory expression with a period of about 2 hours (19,20). Therefore, we decided to use Ub-luc to assess the significance of introns (Fig. 1B).

Transgenic mice carrying either the pH7-UbLuc-In(−) or pH7-UbLuc-In(+) reporter were generated, and explants of dorsal parts of E10.5 embryos were cultured. Time-lapse imaging of the reporter expression was done by monitoring bioluminescence with a highly sensitive CCD camera. Bioluminescence from both pH7-UbLuc-In(−) and pH7-UbLuc-In(+) explant cultures oscillated dynamically (Supplemental Movies 1 and 2), and each cycle corresponded to formation of a bilateral pair of somites (Fig. 1C,D). Reporter expression from both cultures was propagated from the posterior to the anterior PSM, indicating that expression of both reporters accurately reflected endogenous *Hes7* expression. However, we noticed that the timing of the reporter expression was different between the two constructs.

Introns delay the timing of gene expression

We next compared the timing of reporter expression with that of endogenous *Hes7* transcription and of Hes7 protein expression. *Hes7* transcription was examined by in situ hybridization with the first intron probe, as previously described (13). Because expression domains move periodically from the posterior to the anterior PSM, the difference in timing was reflected by the difference in the position of expression domains. The length difference between the anterior ends of expression domains was transformed into a time difference by calculating the propagation speed of the time-lapse imaging of *Hes7* reporter expression (Supplemental Fig. S1).

Reporter expression from pH7-UbLuc-In(−) mice occurred 1.2 min to 17.0 min (on average 10 ± 2 min) more slowly than the endogenous *Hes7* intron expression (Fig. 2A-C,M) but 17.4 min to 23.0 min (on average 21 ± 2 min) earlier than the endogenous Hes7 protein expression (Fig. 2D-F,M). Thus, reporter expression from

pH7-UbLuc-In(–) occurred temporally between the endogenous *Hes7* transcription and Hes7 protein expression (Fig. 2M). In contrast, reporter expression from pH7-UbLuc-In(+) mice occurred 19.4 min to 34.0 min (on average 29 ± 5 min) more slowly than the endogenous *Hes7* intron expression (Fig. 2G-I,M) but 1.7 min to 4.6 min (on average 3 ± 2 min) earlier than the endogenous Hes7 protein expression (Fig. 2J-M). Thus, reporter expression from pH7-UbLuc-In(+) was very similar to the endogenous Hes7 protein expression in timing (Fig. 2M); indeed, it occurred on average about 19 min more slowly than did reporter expression from pH7-UbLuc-In(–). These results suggest that the introns caused a ~19-min delay in Hes7 expression, which was within the expected range of in vivo splicing kinetics (21,22). The ratio of this delay to the segmentation period is comparable to that of zebrafish (23).

To measure the intronic delay in a different system, we transfected the same reporters but under the control of *Hes1* promoter instead of *Hes7* promoter into cultured fibroblasts, because *Hes1* promoter, but not *Hes7* promoter, was active in these cells (Supplemental Fig. S2). We found that the introns led to a similar delay in appearance of the reporter expression (Supplemental Fig. S2). These results confirmed that introns produce a substantial delay in gene expression.

We also noticed that the amplitude of the Hes7 reporter oscillation was different depending on whether the introns were present or not (Fig. 1C,D). Smaller amplitude of pH7-UbLuc-In(+) expression could be due to nonsense-mediated mRNA decay because the stop codon was present in the first exon. To prevent this decay, we performed explant cultures for the pH7-UbLuc-In(+) reporter in the presence of PTC124 (24), but the patterns were not improved (Supplemental Fig. S3). Alternatively, smaller amplitude of pH7-UbLuc-In(+) expression could be due to distributed intronic delays (see Mathematical modeling in supplemental data and Supplemental Fig. S4D).

Hes7 gene introns are required for periodic somite segmentation

We previously proposed a mathematical model consisting of differential equations (see Materials and Methods in Supplemental Data), which accurately described the dynamics of Hes7 oscillations (Supplemental Fig. S4A) (17). Based on this modeling, we found that a 19-min shorter delay would abolish Hes7 oscillations (Supplemental Fig. S4C), although different models predict sustained oscillations without delays (12,18).

To determine whether intronic delays are required for sustained oscillations of

Hes7 expression, we decided to remove all introns from the *Hes7* locus. A targeting vector with the intron-less *Hes7* gene was introduced into mouse ES cells, and homologous recombinants were obtained (Supplemental Fig. S5). After the neo gene was deleted by the Cre-LoxP system, the recombinant ES cells were used to make chimeric mice. From these mice, we obtained homozygous mutant mice carrying the *Hes7* locus whose introns were removed (ΔIn/ΔIn, Fig. 3 and Supplemental Fig. S6). In these intron-less mice, somites were irregular in size and partially fused (Fig. 3B), compared to the wild type (Fig. 3A), indicating that somites were not properly segmented without *Hes7* gene introns. These defects were indistinguishable from *Hes7*-null mice (Fig. 3C). Furthermore, expression of *Tbx18* and *Uncx4.1*, markers for the anterior- and posterior-half somite respectively, was not properly segmented (Fig. 3E, compare with wild type in Fig. 3D, and Supplemental Fig. S7A-D), and the vertebrae and ribs, which are derived from somites, were also severely fused in the intron-less mice (Fig. 3G, compare with the wild type in Fig. 3F). These results indicate that introns in the *Hes7* locus play an essential role in periodic somite segmentation.

<u>*Hes7* gene introns are required for oscillatory expression</u>

To determine the role of intronic delays in oscillatory expression, we next examined the dynamics of cyclic genes in the intron-less mice. Wild-type embryos displayed different patterns of *Hes7* transcription, *Hes7* mRNA expression and Hes7 protein expression, suggesting that *Hes7* expression oscillates in the PSM (Fig. 4A-C,F-H,J-L). Similarly, *Lunatic fringe* (*Lfng*), a gene for a glycosyltransferase of Notch, and *Dusp4*/*MKP2*, a phophatase gene downstream of Fgf signaling, whose expression is regulated by Hes7 oscillations, displayed different expression patterns in the PSM of wild-type embryos (Fig. 4O-Q and Supplemental Fig. S7E). It has been shown that oscillatory expression of *Lfng* is essential for somite segmentation (25-28). In *Hes7*-null mice, however, intron regions of *Hes7* were constitutively expressed throughout the PSM (Fig. 4E) but no Hes7 protein was expressed (Fig. 4N), as previously described (13). In contrast, in the intron-less mice, both *Hes7* mRNA and Hes7 protein were steadily expressed in the PSM (Fig. 4I,M). Furthermore, *Lfng* and *Dusp4*/*MKP2* expression was also steady (Fig. 4R and Supplemental Fig. S7E). *Axin2* expression was still variable but less dynamic in *Hes7* intron-less mice (Supplemental Fig. S7F). In these mice, *Hes7* intron signals were not detectable, confirming that introns were deleted from the *Hes7* locus (Fig. 4D). We

also introduced pH7-UbLuc-In(+) reporter into *Hes7* intron-less mice, but oscillatory reporter expression was not detectable (Supplemental Fig. S8). These results indicate that Hes7 expression does not oscillate; rather, it occurs steadily in the PSM when introns are deleted from the *Hes7* locus.

Introns are known to play an important role in regulating gene expression levels (29). We thus examined Hes7 protein expression levels in the PSM. Extracts of posterior parts of embryos were subjected to western blot analysis. The intron-less mice (ΔIn/ΔIn) expressed about 34% of wild-type levels (Supplemental Fig. S9). It was previously shown that oscillatory expression was maintained in the chick PSM even though more than 80% of protein synthesis was blocked by cycloheximide (30). This phenomenon was also mathematically simulated (14). We also observed that cycloheximide treatment did not abolish *Hes7* mRNA oscillations in the mouse PSM (Supplemental Fig. S10). All these data suggest that loss of Hes7 oscillations are not due to a reduced expression level but to a lack of intronic delays.

Heterozygous mutant mice (+/ΔIn) had normal vertebrae and ribs but displayed a kinked tail, indicating that segmentation defects occurred only at later stages. This late defect is probably because the wild-type allele, which expresses a higher level of Hes7 protein, is dominant over the intron-less allele. To overcome the expression level, multiple copies of the intron(+) and intron-less *Hes7* transgenes (Fig. 5A) were introduced into *Hes7*-null mice. We generated four independent lines carrying the intron(+) *Hes7* transgene and four independent lines carrying the intron-less *Hes7* transgene that expressed Hes7 protein at levels comparable to or higher than the wild type in the PSM (two lines for each transgene were shown in Fig. 5G). All the lines carrying the intron(+) *Hes7* transgene successfully rescued the defect of *Hes7*-null mice (one line was shown in Fig. 5D), whereas all the lines carrying the intron-less *Hes7* transgene failed to rescue the segmentation defects of *Hes7*-null mice (one line was shown in Fig. 5E). Furthermore, the intron-less *Hes7* transgene caused segmentation defects even in the wild-type background (one line was shown in Fig. 5F). These results support the idea that the intronic delay but not the expression level is important for Hes7 oscillations.

Significance of intronic delays in oscillatory expression

The Hes7 reporter without any introns directed reporter expression about 19 min earlier

than the reporter with introns, indicating that introns cause a 19-min delay in the timing of gene expression. Our mathematical modeling predicted that a delay 19 min shorter than the wild type would abolish Hes7 oscillations. We demonstrated that Hes7 oscillations were indeed abolished in embryos carrying the *Hes7* locus whose introns were removed, indicating that introns are essential for Hes7 oscillations. It has been shown that introns and splicing are important for gene expression levels, and we found that only 34% of the wild-type levels of Hes7 protein was expressed in the intron-less mice. However, reduction to the 34% level did not seem to be responsible for loss of oscillations because oscillations were not damped even though more than 80% of protein synthesis was blocked (31). Moreover, we showed that the segmentation defects of *Hes*7-null mice were rescued by introduction of multiple copies of the intron(+) *Hes7* transgene but not by introduction of the intron-less *Hes7* transgene, although the Hes7 expression levels were rescued. All these data suggest that intronic delays, but not intron/splicing-dependent gene expression levels, are important for sustained Hes7 oscillations.

Our current mathematical modeling also predicted that the instability of Hes7 gene products is essential for sustained oscillations, and that if the products are stabilized, oscillations would be damped (17). We previously demonstrated that Hes7 oscillations are indeed damped in embryos with a point mutation that makes the Hes7 protein half-life about 8 min longer than the wild type (17). Thus, we have to date evaluated two important predictions of our mathematical modeling: that the instability of gene products and sufficient delays in the timing of gene expression are required for sustained oscillations (14-16), and verified both predictions by introducing specific mutations into mouse embryos. Taken together, our current mathematical modeling, which is based on delayed negative feedback, accurately describes the dynamics of Hes7 oscillations. However, recent studies have revealed that multiple signaling molecules are involved in oscillatory expression in the PSM (11,31), and incorporation of such oscillators will be required to understand the whole structure of the segmentation clock.

Materials and methods

Hes7 reporter mice

The reporters consisted of the genomic fragment of *Hes7* promoter region (5393-bp upstream fragment from the first codon), firefly luciferase gene fused with human ubiquitin variant (G76V) with a termination codon (TAA) at the 3'-end (19), and a genomic sequence from the second codon to 76-bp downstream of the putative polyadenylation signal. For pH7-UbLuc-In(−), all introns were removed. Transgenic mice were generated by injecting the linearized constructs without any vector sequence into the pronucleus of fertilized eggs. All animals used for this study were maintained and handled according to protocols approved by Kyoto University.

Bioluminescence imaging of the PSM

All images were recorded in 16 bit with IMAGE-PRO PLUS (Media Cybernetics, Silver Spring, MD), and other equipments were described previously (19) with following modifications. To increase the number of samples at a single capturing, 10x UPlan FLN (NA 0.30) objective lens was used with 4x4 binning and exposure of 10 min. Tyrode's solution was used when dissecting embryos and capturing images. For movies, recording was performed, as previously described (19). Briefly, 20x UPlan Apo Objective (NA 0.80) was used with 4x4 binning and exposure of 19 min 24 sec. For processing of bioluminescence images, cosmic ray-induced signals were first removed, and then the images were converted to 8-bit with 1024x1024 in size by setting the maximum intensity to 255 and the minimum to zero. The 8-bit images of the PSM were aligned in the same anterior-posterior axis by Photoshop (Adobe Systems Inc.) to correct the moving of the tissue during recording. The images were trimmed into 15 pixels in width.

Generation of the intron-less *Hes7* mutant mice

The targeting vector was constructed by replacing the *Hes7* coding and intron region with *Hes7* cDNA to remove all introns. Floxed Neo^r cassette was inserted into the SacI site in the 3'-downstream region of *Hes7*, while diphtheria toxin A gene was ligated to the 3'-homologous region of the vector (Supplemental Fig. 4A). The vector was electroporated into TT2 embryonic stem (ES) cells, and G418-resistant clones were analyzed by southern blotting to isolate homologous recombinant ES cells. Neo^r cassette was next removed by transient expression of Cre recombinase. Chimeras were

generated by injecting recombinant ES cells into 8-cell stage ICR embryos according to standard procedures.

Genotyping and analysis of mice

Genomic DNA was prepared from either tails of adult mice or amnion of embryos. Genotypes were determined by PCR. Primer sequences are described in Supplemental Data. Whole-mount in situ hybridization and whole-mount immunochemistry were performed, as described previously (13). Cartilage and bone of neonates were stained with alcian blue and alizarin red, respectively, as described previously (10).

Western blotting

The posterior parts of embryos were mixed with 30μl of lysis buffer (50mM Tris-HCl pH8.0, 100mM NaCl, 5mM $MgCl_2$, 0.5% NP-40, 1xProteinase inhibitor cocktail, 1mM PMSF, 250U/ml Benzonase) and incubated on ice for 30 min. After addition of 3μl of 10% SDS, the samples were boiled, and the protein concentrations were measured. The protein solution after boiled in sample buffer was run on 12.5% SDS-PAGE. After transferring protein from the gel to PVDF membrane (Millipore #IPVH15150), the membrane was immersed in buffer containing 5% skim milk, anti-Hes7 antibody (1/500, 13), and peroxidase-conjugated anti-guinea pig IgG (1/5000, Chemicon) in sequence. Immunoreactive bands were visualized with ECL-plus (GE healthcare) and LAS 3000mini (Fuji film). Intensity of each band was calculated with Image Gauge (Fuji film). After stripping of antibodies, the membrane was immersed in buffer containing 5% skim milk, anti-β-tubulin IgG (Santa Cruz), and peroxidase conjugated anti-rabbit IgG (GE healthcare) in sequence. Immunoreactive bands were visualized with ECL (GE healthcare).

Acknowledgements

We thank A. Isomura for discussion. This work was supported by the Genome Network Project and the Grants-in-aid from the Ministry of Education, Culture, Sports, Science and Technology of Japan, and the Uehara Memorial Foundation. Y.T. was supported by the 21st Century COE Program of the Ministry of Education, Culture, Sports, Science

and Technology of Japan.

References

1. Thummel CS (1992) Mechanisms of transcriptional timing in *Drosophila*. *Science* **255:** 39-40.
2. Swinburne IA, Silver PA (2008) Intron delays and transcriptional timing during development. *Dev Cell* **14:** 324-330.
3. Swinburne IA, Miguez DG, Landgraf D, Silver PA (2008) Intron length increases oscillatory periods of gene expression in animal cells. *Genes Dev* **22:** 2342-2346.
4. Saga Y, Takeda H (2001) The making of the somite: molecular events in vertebrate segmentation. *Nat Rev Genet* **2:** 835-845.
5. Aulehla A, Herrmann BG (2004) Segmentation in vertebrates: clock and gradient finally joined. *Genes Dev* **18:** 2060-2067.
6. Giudicelli F, Lewis J (2004) The vertebrate segmentation clock. *Curr Opin Genet Dev* **14:** 407-414.
7. Kageyama R, Ohtsuka T, Kobayashi T (2007) The Hes gene family: repressors and oscillators that orchestrate embryogenesis. *Development* **134:** 1243-1251.
8. Mara A, Holley SA (2007) Oscillators and the emergence of tissue organization during zebrafish somitogenesis. *Trends Cell Boil* **17:** 593-599.
9. Dequéant M-L, Pourquié O (2008) Segmental patterning of the vertebrate embryonic axis. *Nat Rev Genet* **9:** 370-382.
10. Bessho Y et al (2001) Dynamic expression and essential functions of *Hes7* in somite segmentation. *Genes Dev* **15:** 2642-2647.
11. Niwa Y et al (2007) The initiation and propagation of Hes7 oscillation are cooperatively regulated by Fgf and Notch signaling in the somite segmentation clock. *Dev Cell* **13:** 298-304.
12. Hirata H et al (2002) Oscillatory expression of the bHLH factor Hes1 regulated by a negative feedback loop. *Science* **298:** 840-843.
13. Bessho Y, Hirata H, Masamizu Y, Kageyama R (2003) Periodic repression by the bHLH factor Hes7 is an essential mechanism for the somite segmentation clock.

Genes Dev **17:** 1451-1456.

14. Lewis J (2003) Autoinhibition with transcriptional delay: a simple mechanism for the zebrafish somitogenesis oscillator. *Curr Biol* **13:** 1398-1408.
15. Monk NAM (2003) Oscillatory expression of Hes1, p53, and NF-kB driven by transcriptional time delays. *Curr Biol* **13:** 1409-1413.
16. Jensen MH, Sneppen K, Tiana G (2003) Sustained oscillations and time delays in gene expression of protein Hes1. *FEBS Lett* **541:** 176-177.
17. Hirata H et al (2004) Instability of Hes7 protein is crucial for the somite segmentation clock. *Nat Genet* **36:** 750-754.
18. Tiedemann HB et al (2007) Cell-based simulation of dynamic expression patterns in the presomitic mesoderm. *J Theor Biol* **248:** 120-129.
19. Masamizu Y et al (2006) Real-time imaging of the somite segmentation clock: revelation of unstable oscillators in the individual presomitic mesoderm cells. *Proc Natl Acad Sci USA* **103:** 1313-1318.
20. Shimojo H, Ohtsuka T, Kageyama R (2008) Oscillations in Notch signaling regulate maintenance of neural progenitors. *Neuron* **58:** 52-64.
21. Audibert A, Weil D, Dautry F (2002) In vivo kinetics of mRNA splicing and transport in mammalian cells. *Mol Cell Biol* **22:** 6706-6718.
22. Singh J, Padgett RA (2009) Rates of *in situ* transcription and splicing in large human genes. *Nat Struct Mol Biol* **16:** 1128-1133.
23. Giudicelli F, Özbudak EM, Wright GJ, Lewis J (2007) Setting the tempo in development: an investigation of the zebrafish somite clock mechanism. *PLoS Biol* **5:** e150.
24. Welch EM et al (2007) PTC124 targets genetic disorders caused by nonsense mutations. *Nature* **447:** 87-91.
25. Evrard YA, Lun Y, Aulehla A, Gan L, Joonson RL (1998) *lunatic fringe* is an essential mediator of somite segmentation and patterning. *Nature* **394:** 377-381.
26. Zhang N, Gridley T (1998) Defects in somite formation in lunatic fringe-deficient mice. *Nature* **394:** 374-377.
27. Serth K, Schuster-Gossler K, Cordes R, Gossler A (2003) Transcriptional oscillation of Lunatic fringe is essential for somitogenesis. *Genes Dev* **17:** 912-925.
28. Shifley E, VanHorn KM, Perez-Balaguer A, Franklin JD, Weinstein M, Cole SE (2007) Oscillatory lunatic fringe activity is crucial for segmentation of the anterior

but not posterior skeleton. *Development* **135:** 899-908.

29. Tange ØT, Nott A, Moore MJ (2004) The ever-increasing complexities of the exon junction complex. *Curr Opin Cell Biol* **16:** 279-284.
30. Palmeirim I, Henrique D, Ish-Horowicz D, Pourquié O (1997) Avian *hairy* gene expression identifies a molecular clock linked to vertebrate segmentation and somitogenesis. *Cell* **91:** 639-648.
31. Dequéant M-L, Glynn E, Gaudenz K, Wahl M, Chen J, Mushegian A, Pourquié O (2006) A complex oscillating network of signaling genes underlies the mouse segmentation clock. *Science* **314:** 1595-1598.

Figure Legends

Figure 1. Dynamic expression of the intron (+) and intron (−) *Hes7* reporters. (*A*) Schematic view of *Hes7* transcription and Hes7 protein expression in the presomitic mesoderm. *Hes7* transcription and Hes7 protein expression occur in a mutually exclusive manner. (*B*) *Hes7* reporter gene constructs. *Hes7* promoter-driven firefly luciferase gene fused with human ubiquitin variant (G76V) was used as a reporter. pH7-UbLuc-In(−) has no intron, while pH7-UbLuc-In(+) has all introns. The total size of three introns is 1,843 bp. (*C,D*) The left panels show reporter expression from pH7-UbLuc-In(−) (*C*) and pH7-UbLuc-In(+) (*D*). The middle panels show the spatiotemporal profiles of the reporter expression measured along the vertical red line in the left panels. The right panels show quantification of the reporter expression. The signal intensity was measured at the middle region of the PSM (indicated by arrowheads in the middle panels). Similar expression patterns were observed in four independent experiments for each reporter.

Figure 2. Introns delay the timing of *Hes7* reporter expression. (*A–L*) Comparison of reporter expression (Luc) with either *Hes7* intron expression or Hes7 protein expression in pH7-UbLuc-In(−) mice (*A–F*) or pH7-UbLuc-In(+) mice (*G–L*). Reporter expression was classified into three phases based on luciferase activity. Phase A: Relatively narrower expression in the anterior PSM and broader expression in the posterior PSM

(*A,D,G,J*). Phase B: Strong expression in the middle part of the PSM (*B,E,H,K*). Phase C: Relatively broader expression in the anterior PSM and narrower expression in the posterior PSM (*C,F,I,L*). After acquisition of luciferase activity images, posterior parts of the embryos were fixed immediately and analyzed for either *Hes7* intron expression (n = 16 in *A–C*, n = 7 in *G–I*) or Hes7 protein expression (n = 22 in *D–F*, n = 22 in *J–L*). The first column shows bright field (BF) images. The difference in space (1 unit is defined as a one somite length) was converted into the difference in time based on the movies. The averages with standard errors are shown. Arrowhead on the left side of each panel indicates a boundary between a newly-formed somite and the PSM. (*M*) Comparison of *Hes7* reporter expression with *Hes7* gene transcription and Hes7 protein expression.

Figure 3. Segmentation defects in mice carrying the intron-less *Hes7* alleles. (*A–C*) Bright field images of E8.5 embryos. Somites were regular in size and symmetric between the left and right in wild type (A) but not in intron-less (ΔIn/ΔIn, *B*) and *Hes7*-null mice (Null/Null, *C*). (D,E) *Uncx4.1* expression in E9.5 embryos. Somites were severely fused in *Hes7* intron-less mice (ΔIn/ΔIn, *E*). (*F*,*G*) Bones and cartilages of neonates were stained in red and blue, respectively. The vertebrae and ribs were severely fused in the intron-less mice (*G*).

Figure 4. Oscillatory expression was abolished in mice carrying the intron-less *Hes7* alleles. There were different patterns of *Hes7* gene transcription (n = 16, *A–C*), which were detected by intron in situ hybridization, *Hes7* mRNA expression (n = 3, *F–H*), Hes7 protein expression (n = 13, *J–L*) and *Lfng* mRNA expression (n = 5, *O–Q*) in E10.5 wild-type embryos (WT). This suggested that *Hes7* and *Lfng* expression oscillates in the WT. In contrast, *Hes7* intron signals were undetectable in the intron-less mice (n = 6, ΔIn/ΔIn, *D*) but were observed steadily in the PSM of *Hes7*-null mice (n = 13, Null/Null, *E*) at E10.5. Furthermore, *Hes7* mRNA was expressed steadily in the PSM of the intron-less mice (n = 4, ΔIn/ΔIn, *I*). In addition, Hes7 protein was steadily expressed in the PSM of intron-less mice (n = 10, ΔIn/ΔIn, *M*) but not detectable in the PSM of *Hes7*-null mice (n = 8, Null/Null, *N*). *Lfng* mRNA was also expressed steadily in the PSM of the intron-less mice (n = 4, ΔIn/ΔIn, *R*).

Figure 5. Segmentation defects of *Hes7*-null mice were rescued by intron(+) *Hes7* transgene but not by intron(−) *Hes7* transgene. (*A*) Structures of intron(+) and intron(−) *Hes7* transgenes. HA tag was added to the amino-terminus to differentiate between the endogenous and transgene expression. This tag did not affect the segmentation (see *D*). (*B*) Wild-type mouse. (*C*) *Hes7*-null mouse. (*D*) *Hes7*-null mouse containing the intron(+) *Hes7* transgene. Four independent lines containing the intron(+) *Hes7* transgene including the one shown here (line 2) rescued the segmentation defects. (E) *Hes7*-null mouse containing the intron(−) *Hes7* transgene. Four independent lines containing the intron(−) *Hes7* transgene including the one shown here (line 4) did not rescue the segmentation defects. (F) Segmentation defects were caused even in the *Hes7*(+/+) backgroud by the intron(−) *Hes7* transgene (line 3). Bones and cartilages of neonates were stained in red and blue, respectively (*B-F*). (*G*) Western blot analysis of the PSM in the *Hes7*(+/+) background. Hes7 protein levels in two independent lines of the intron(+) transgene (lines 1 & 2) and two independent lines of the intron(−) transgene (lines 3 & 4) were shown. Hes7 protein made from the transgene is larger in size than the endogenous one because of the HA tag. β-tubulin was used as a control. Note that the endogenous Hes7 protein expression was down-regulated by the exogenous Hes7 protein expressed from the transgenes. Segmentation defects of *Hes7*-null mice were rescued by the intron(+) transgene lines 1 and 2 but not by the intron(−) transgene lines 3 and 4.

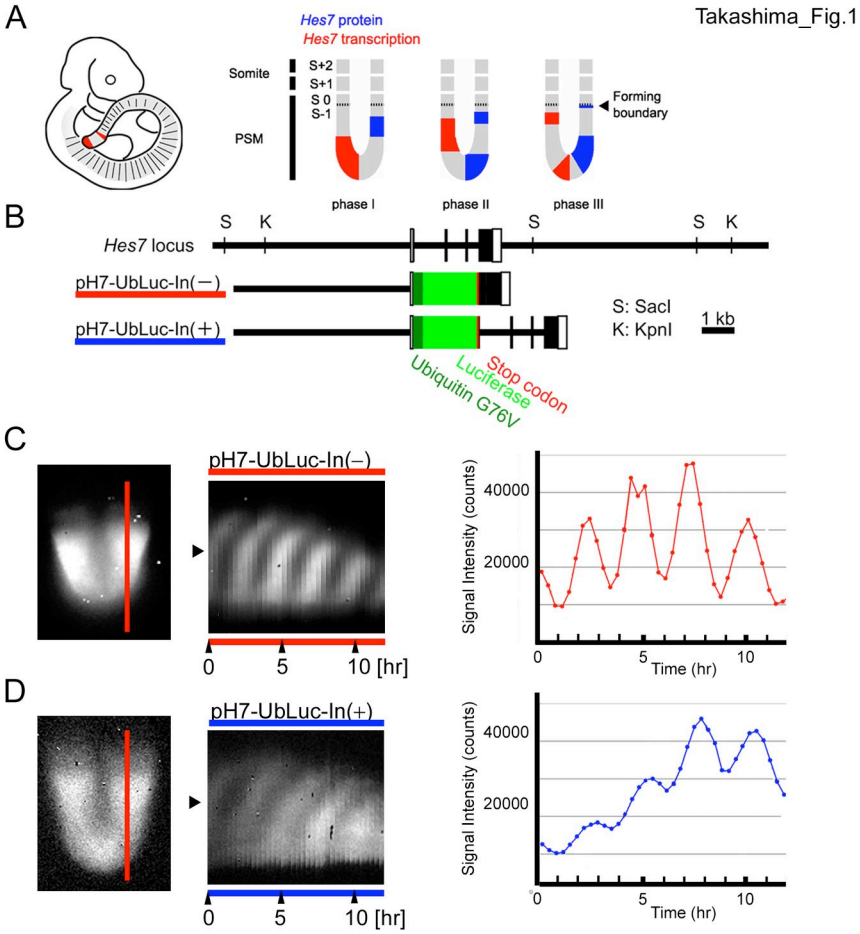
A
Takashima_Fig.1
Hes7 protein
Hes7 transcription
Somite
PSM
S+2
S+1
S 0
S-1
Forming boundary
phase I
phase II
phase III
B
S K
S
S K
Hes7 locus
pH7-UbLuc-ln(−)
pH7-UbLuc-ln(+)
S: SacI
K: KpnI
1 kb
Stop codon
Luciferase
Ubiquitin G76V
C
pH7-UbLuc-ln(−)
0
5
10 [hr]
Signal Intensity (counts)
40000
20000
0
5
10
Time (hr)
D
pH7-UbLuc-ln(+)
0
5
10 [hr]
Signal Intensity (counts)
40000
20000
0
5
10
Time (hr)

Takashima_Fig.2

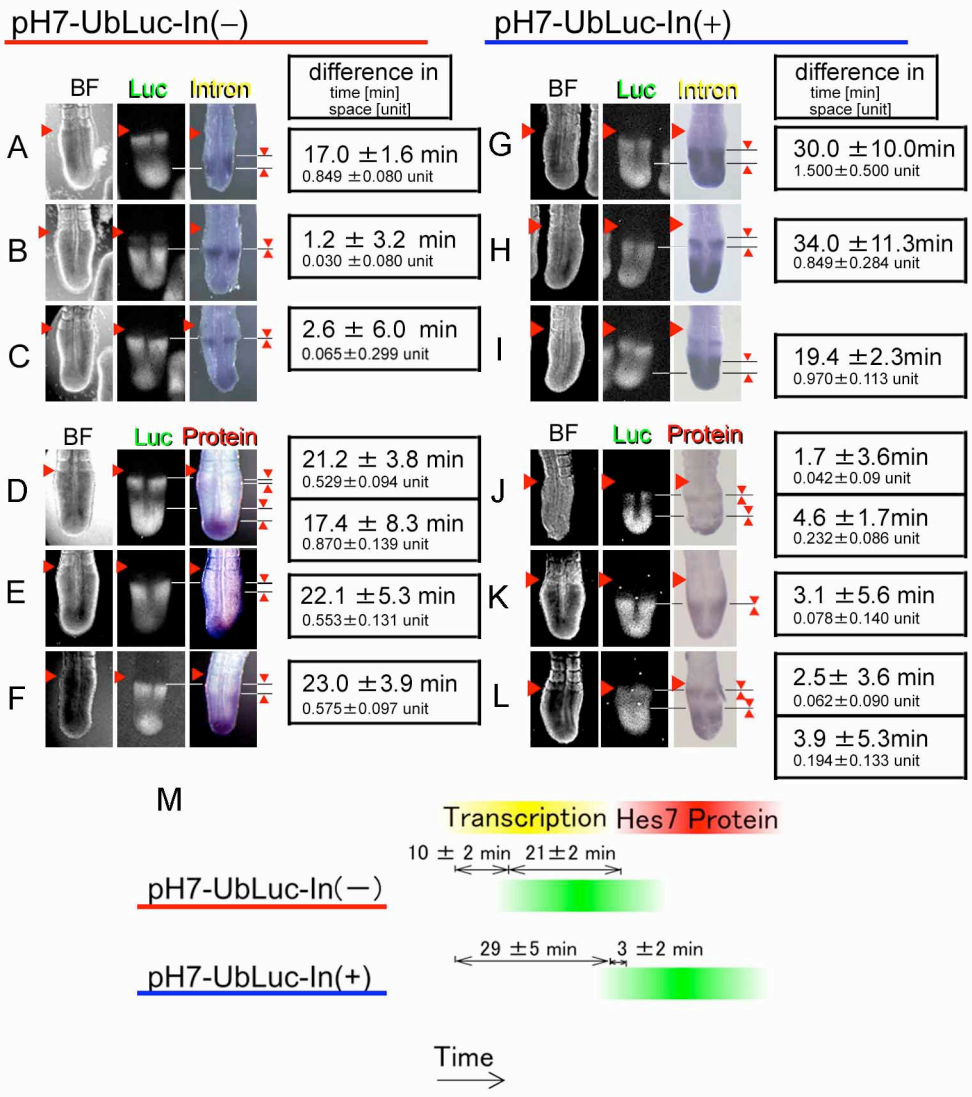

Figure 2

Takashima_Fig.3

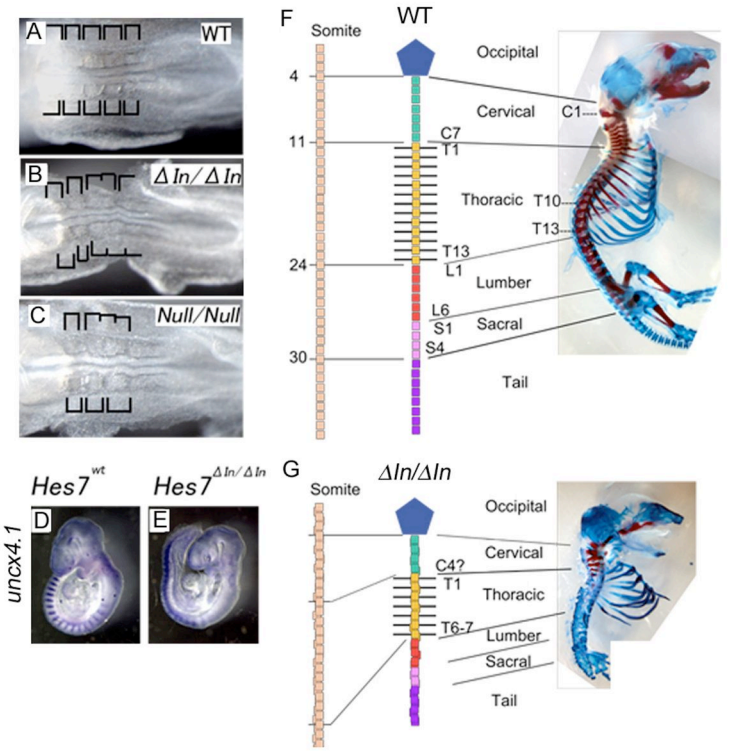

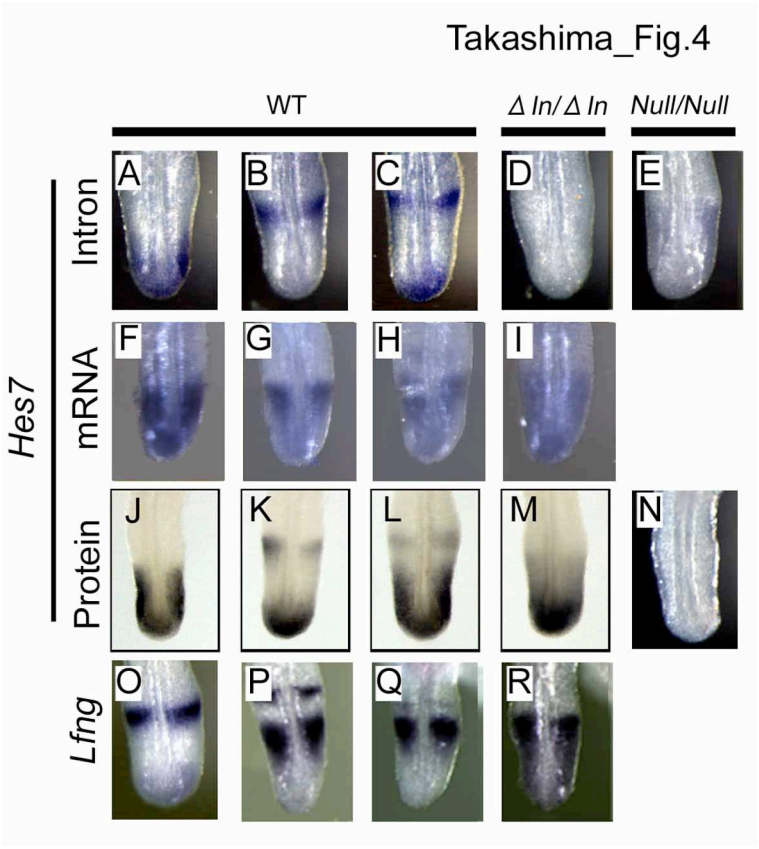
Takashima_Fig.4
WT
Δ In/Δ In
Null/Null
Hes7
Intron
mRNA
Protein
Lfng
A
B
C
D
E
F
G
H
I
J
K
L
M
N
O
P
Q
R

Takashima_Fig.5

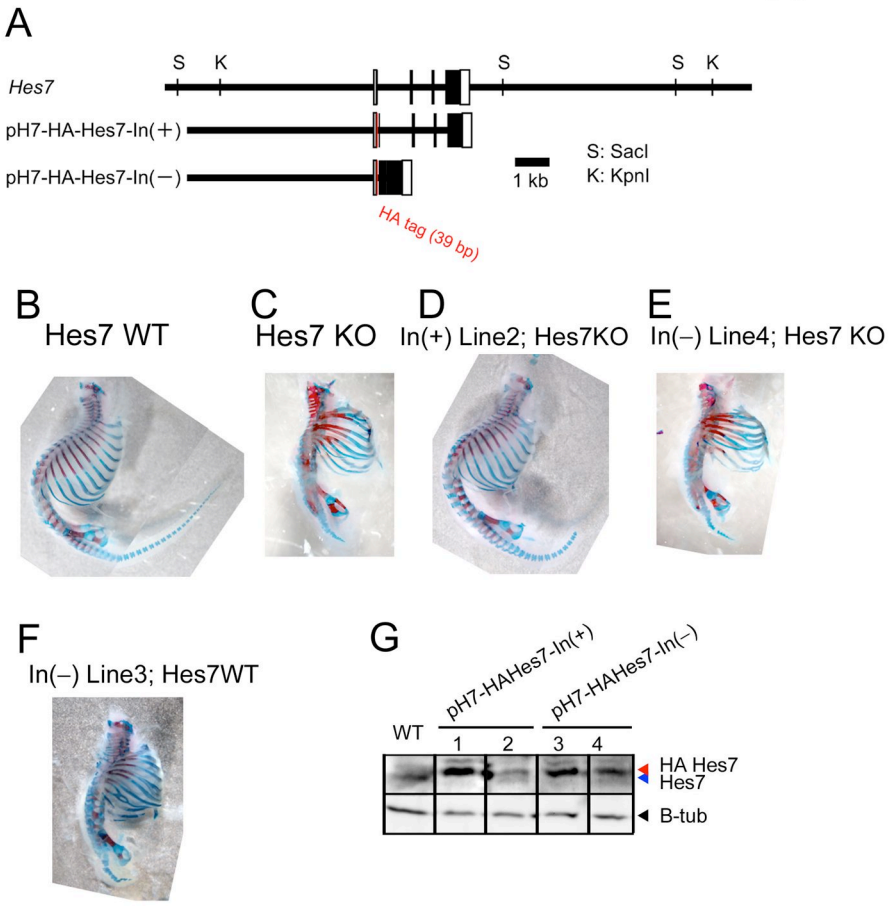

Supplemental Data

Materials and Methods

Measurement of time delays

The velocity of movement of the luciferase expression domain relative to the posterior tip of the PSM was measured from the spatiotemporal profiles of Supplemental movie 1 (Supplemental Fig. S1) so that the space distance can be converted into the time distance. The propagation speed was found to be about 1 unit/20min (= 0.05 unit/min) during phase A and 1 unit/40min (= 0.025 unit/min) during phases B and C. 1 unit is defined as one somite length. For definition of phases A-C, see Fig. 2 legend. To determine the space distance between the reporter expression and *Hes7* transcription, the PSM samples were subjected to in situ hybridization with the first intron as a probe after imaging of reporter expression. To determine the space distance between the reporter expression and Hes7 protein expression, the PSM samples were subjected to immunostaining with Hes7 antibody after imaging of reporter expression. Because the expression domains were propagated into the anterior region, the distance from the last somite border to the anterior end of the reporter, the intron and Hes7 protein expression was measured. During in situ hybridization and immunostaining, the size of the PSM was changed and therefore normalized to the original size. The distance between the anterior ends of the reporter expression and the intron/Hes7 protein expression was measured and then converted into the time difference based on the propagation speed.

Mathematical simulation: significance of delays

Hes7 oscillations are simulated with the following equations (1):

$$\frac{dp(t)}{dt} = am(t - T_p) - bp(t)$$

$$\frac{dm(t)}{dt} = f(p(t - T_m)) - cm(t)$$

where $p(t)$ and $m(t)$ are the quantities of functional Hes7 protein and *Hes7* mRNA per cell at time t, respectively, and $f(p)$ is the rate of initiation of transcription, which

depends on the amount of the protein, p, present at the time of initiation. a is the rate constant for translation, while b and c are the degradation rate constants for Hes7 protein and *Hes7* mRNA, respectively, which are simply related to the half-lives of the molecules:

$$b = \frac{\ln 2}{\tau_p}, \quad c = \frac{\ln 2}{\tau_m}$$

Because transcription is inhibited by Hes7 protein, which acts as a dimer, we assume

$$f(p) = \frac{k}{1 + (\frac{p}{p_{crit}})^2}$$

where k is the number of molecules of *Hes7* mRNA synthesized per unit time in the absence of inhibition and p_{crit} is the amount of protein that gives half-maximal inhibition. We set a = 4.5 protein molecules per mRNA molecule per min, p_{crit} = 40 molecules per cell, k = 33 mRNA molecules per cell per min, τ_m = 3 min. We assume that the Hes7 protein half-life τ_p = 20 min, T_p = 8 min, and T_m = 29 min. Under these conditions, oscillatory expression continues (Supplemental Fig. S3A). In contrast, when T_m = 10 min (19 min shorter), oscillations are abolished (Supplemental Fig. S3C).

Mathematical simulation: distributed delays

The amplitude of the Hes7 reporter oscillation was different depending on whether the introns were present or not (Fig. 1C,D). We hypothesized that the cause of these differences is related to the nature of the introns (discrete vs. distributed). The average signal of both reporters seemed to increase, at least during the first three peaks. On the other hand, the amplitude seemed to be significantly different between pH7-UbLuc-In(+) and pH7-UbLuc-In(-). In pH7-UbLuc-In(-) reporter, the average signal was around 2E+4 at 3h and around 3E+4 at 5h, so that there was an approximate increase of 0.5-fold units every hour. In pH7-UbLuc-In(+) reporter, the average signal was around 1.5E+4 at 2h and around 2.5E+4 at 4.5h, so that there was an approximate increase of 0.4-fold units every hour. To model this observation, we hypothesized that this relatively

similar signal increase is due to increasing amounts of luciferase substrate inside the cells (function *s*(*t*) in equation (1)). Regarding the amplitude differences, the amplitude of pH7-UbLuc-In(-) reporter was about 2 fold while the amplitude of pH7-UbLuc-In(+) reporter was about 1 fold. To model this observation, we hypothesized that the intronic delay is distributed around an average value.

We used the previously described model (1) with an additional variable *l* for the luminescence:

$$\begin{aligned} \frac{dp}{dt} &= am(t-T_p) - \frac{ln2}{\tau_p}p(t) \\ \frac{dm}{dt} &= \frac{k}{1+(\frac{p(t-T_m)}{p_{crit}})^2} - \frac{ln2}{\tau_m}m(t) \\ \frac{dl}{dt} &= \frac{ks(t)}{1+(\frac{\int_0^\infty p(t-T_l)g_v^r(T_l)dT_l}{p_{crit}})^2} - \frac{ln2}{\tau_m}l(t) \end{aligned} \qquad (1)$$

The function *s*(*t*) stands for the intracellular luciferase substrate. To account for the distributed delay, we integrated a delayed protein concentration $p(t - T_l)$ weighted with a probability distribution $g_v^r(T_l)$ from $T_l = 0$ to $T_l = \infty$ (2,3). The probability distribution $g_v^r(T_l) = \frac{v^{r+1}}{r!} T_l^r e^{vT_l}$ showed a maximum at $T_l = r/v$ and was zero for $T_l = 0$ and for $T_l \rightarrow \infty$. The value of *r* influenced the shape of the probability distribution $g_v^r(T_l)$ from a broad distribution for low *r* to a very sharp distribution approximating a discrete delay for high *r*. To simulate the integral differential equation, we need to convert it into a set of ordinary differential equations using the linear chain trick (2), which results in:

$$\begin{aligned} \frac{dl}{dt} &= \frac{ks(t)}{1+(\frac{x_r}{p_{crit}})^2} - \frac{ln2}{\tau_m}l(t) \\ \frac{dx_0}{dt} &= v(p(t) - x_0(t)) \\ \frac{dx_j}{dt} &= v(x_{j-1}(t) - x_j(t)),\ j = 1, ..., r \end{aligned} \qquad (2)$$

For $r = 1$ and $v = r/T_l$, the set of equations become:

$$
\begin{aligned}
\frac{dp}{dt} &= am(t-T_p) - \frac{ln2}{\tau_p}p(t) \\
\frac{dm}{dt} &= \frac{k}{1+(\frac{p(t-T_m)}{p_{crit}})^2} - \frac{ln2}{\tau_m}m(t) \\
\frac{dl}{dt} &= \frac{ks(t)}{1+(\frac{x_1}{p_{crit}})^2} - \frac{ln2}{\tau_m}l(t) \qquad (3) \\
\frac{dx_0}{dt} &= \frac{r}{T_l}(p(t)-x_0(t)) \\
\frac{dx_1}{dt} &= \frac{r}{T_l}(x_0(t)-x_1(t))
\end{aligned}
$$

To simulate the previous equation system, we chose the same parameter values as previously described (1), that is: a = 4.5; p_{crit} = 40; k = 33; τ_m = 3; τ_p = 20; T_p = 8; n = 2. For the distributed delay, the parameter is r = 1. We carried out two simulations for the pH7-UbLuc-In(-) and pH7-UbLuc-In(+) case where T_l = 10 min (Fig. 1C) and T_l = 29 min (Fig. 1D), respectively. To remove transient effects, the model was simulated for 9,400 min before plotting. During the transient simulation, the intracellular substrate was held at $s(t)$ = 0 and after that the substrate concentration followed the function $s(t)$ = 0.283t. These results suggest that the increase of the average signal is related to the concentration increase of the intracellular luciferase substrate, while the differences of amplitude between pH7-UbLuc-In(-) and pH7-UbLuc-In(+) constructs are related to the distributed nature of the reporter delay (Supplemental Fig. S3D).

Primers for genotyping

Genotypes were determined by PCR using the following primers.

For pH7-UbLuc-In(+) and pH7-UbLuc-In(-) mice,

LucF: 5'-TACTGGTCTGCCTAAAGGTG-3',

LucR: 5'-CCACCAGAAGCAATTTCGTG-3'.

For wild-type, *Hes7*-null and *Hes7* intron-less mice (see Supplemental Fig. S5),

Primer 1: 5'-GTCACCCGGGAGCGAGCTGAGAAT-3',

Primer 2: 5'-AAGTTGGGCTCTGACCCTGCCCTC-3',

Primer 3: 5'-AGCGCGGAGAAAAGCTGGGAGCGTG-3',

Primer 4: 5'-AGAAAGGGCAGGGAGAAGTGGGCGAGCCAC-3',

Primer 5: 5'-GTTCTGAGAGCGAGAGGGGGTCTGGGATGG-3',

Primer 6: 5'-TTGGCTGCAGCCCGGGGGATCCACTAGTTC-3'.

For rescue experiments with pH7-HA-Hes7-In(+) and pH7-HA-Hes7-In(–), the following primers as well as primers 2, 3 and 5 were used.

Primer 7: 5'-ACCCTGCAGCGGCGGGATATAAGG-3',

Primer 8: 5'-GTCCACCGAAGGGTCCGGAGGAGCAATGGT-3'.

Primers 2, 3 and 7 were used for pH7-HA-Hes7-In(+) (319 bp), pH7-HA-Hes7-In(–) (486 bp), and the wild-type and *Hes7*-null alleles (266 bp). Primers 5 and 8 were used for wild-type endogenous *Hes7* allele.

Western blotting

The posterior parts of embryos were mixed with 30μl of lysis buffer (50mM Tris-HCl pH8.0, 100mM NaCl, 5mM $MgCl_2$, 0.5% NP-40, 1xProteinase inhibitor cocktail, 1mM PMSF, 250U/ml Benzonase) and incubated on ice for 30 min. After addition of 3μl of 10% SDS, the samples were boiled, and the protein concentrations were measured. The protein solution after boiled was run on 12.5% SDS-PAGE. After transferring protein from the gel to PVDF membrane (Millipore #IPVH15150), the membrane was immersed in buffer containing 5% skim milk, anti-Hes7 antibody (1/500) (4), and peroxidase-conjugated anti-guinea pig IgG (1/5000, Chemicon) in sequence. Immunoreactive bands were visualized with ECL-plus (GE healthcare) and LAS 3000mini (Fuji film). Intensity of each band was calculated with Image Gauge (Fuji film). After stripping antibodies, the membrane was immersed in buffer containing 5% skim milk, anti-β-tubulin IgG (Santa Cruz), and peroxidase conjugated anti-rabbit IgG (GE healthcare) in sequence. Immunoreactive bands were visualized with ECL (GE healthcare). The intensity of Hes7 protein was normalized by that of β–tubulin.

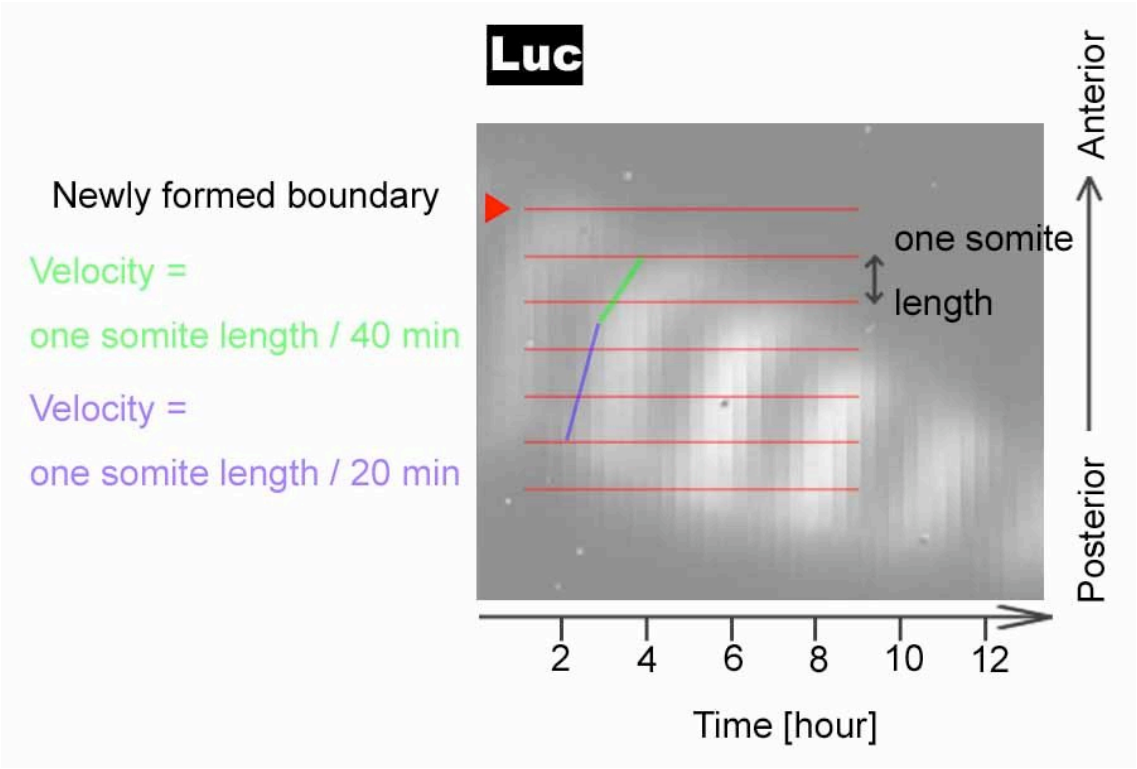

Supplemental Figure S1. Spatiotemporal profiles of *Hes7* oscillations in the PSM. The bioluminescence intensity of pH7-UbLuc-In(−) along the anterior-posterior axis was plotted according to the time. The profiles were made from Supplemental Movie 1. *Hes7* oscillation was propagated from the posterior end to the anterior PSM. The space between red lines corresponds to one somite length. Arrowhead indicates the position of a newly formed boundary around time = 5. Based on the spatiotemporal profiles from Supplemental Movie 1, the velocity of movement of the luciferase expression domain (propagation speed) was measured. The average propagation speed was about 1 unit/20min (= 0.05 unit/min) during phase A and 1 unit/40min (= 0.025 unit/min) during phases B and C. 1 unit is defined as one somite length. For definition of phases A-C, see Fig. 2 legend.

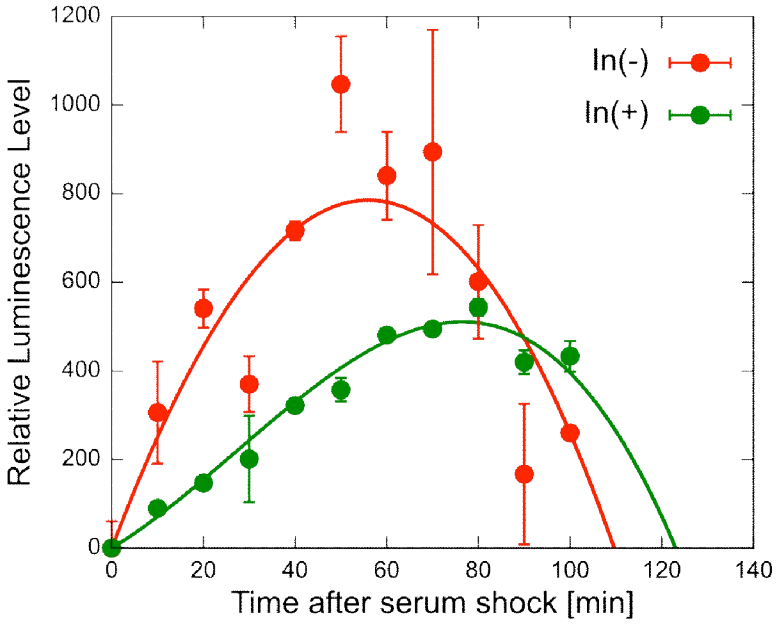

Supplemental Figure S2. Introns delay the timing of gene expression. *Hes1* promoter-driven Ub-Luc reporters, pH1-UbLuc-In(–), which has no intron, and pH1-UbLuc-In(+), which has all *Hes7* gene introns, were transfected into C3H10T1/2 cells, and the reporter protein expression after serum stimulation were quantified. The average peak of Luc occurred at time = 56 min in pH1-UbLuc-In(–) and at time = 77 min in pH1-UbLuc-In(+). Thus, introns led to about 20 min delay in the expression. The average with a standard error of three independent experiments was determined at each time point.

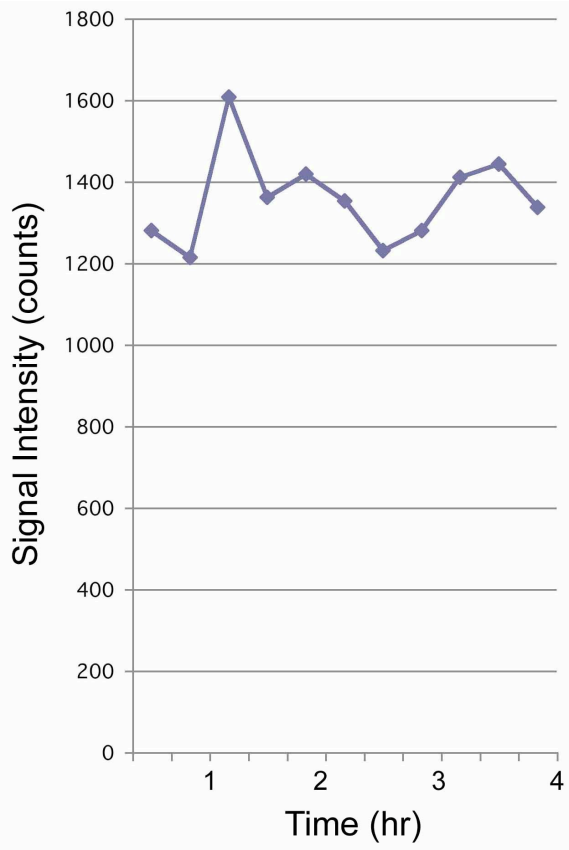

Supplemental Figure S3. pH7-UbLuc-In(+) reporter expression in the presence of PTC124. To prevent nonsense-mediated mRNA decay, the pH7-UbLuc-In(+) reporter explant was cultured in the presence of 0.5μg/ml PTC124 (Enzo Life Sciences). We also performed the culture in the presence of 5.0μg/ml PTC124 and obtained similar patterns. The amplitude was not improved by PTC124.

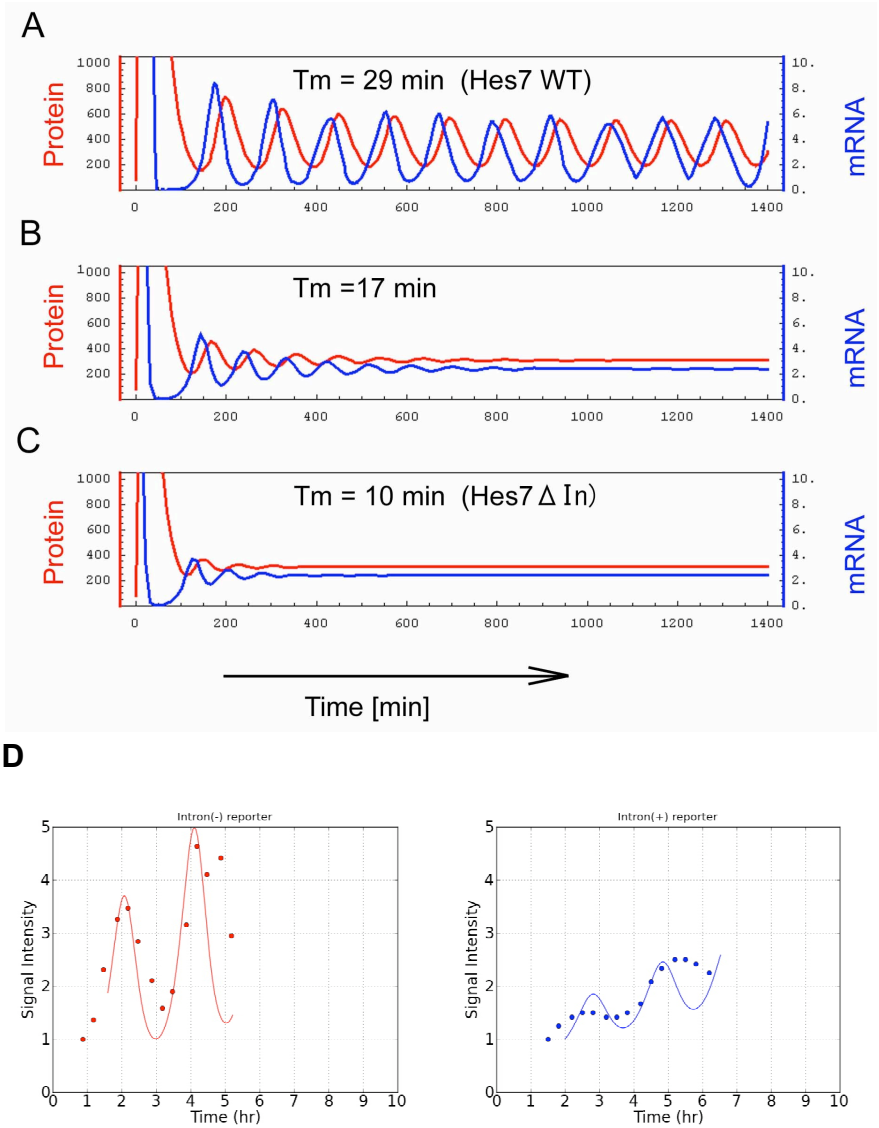

Supplemental Figure S4. Mathematical simulation of *Hes7* mRNA and Hes7 protein oscillations. (*A*) When a transcriptional delay (T_m) is 29 min (the wild-type condition), oscillations of *Hes7* mRNA and Hes7 protein expression continue in a sustained manner (see Materials and Methods of Supplemental Data). (*B*) A 12 min shorter delay (T_m = 17 min) makes the amplitude much smaller and damps oscillatory expression. (*C*) A 19 min shorter delay (T_m = 10 min, the ΔIn/ΔIn condition) abolishes oscillations of *Hes7* mRNA and Hes7 protein expression. (D) Simulation of the pH7-UbLuc-In(-) reporter (T_l = 10 min) (*left panel*) and the pH7-UbLuc-In(+) reporter (T_l = 29 min) (*right panel*). Continuous curves show the simulations while dots stand for experimental data. The simulation values were normalized by dividing with the minimal value of the simulation.

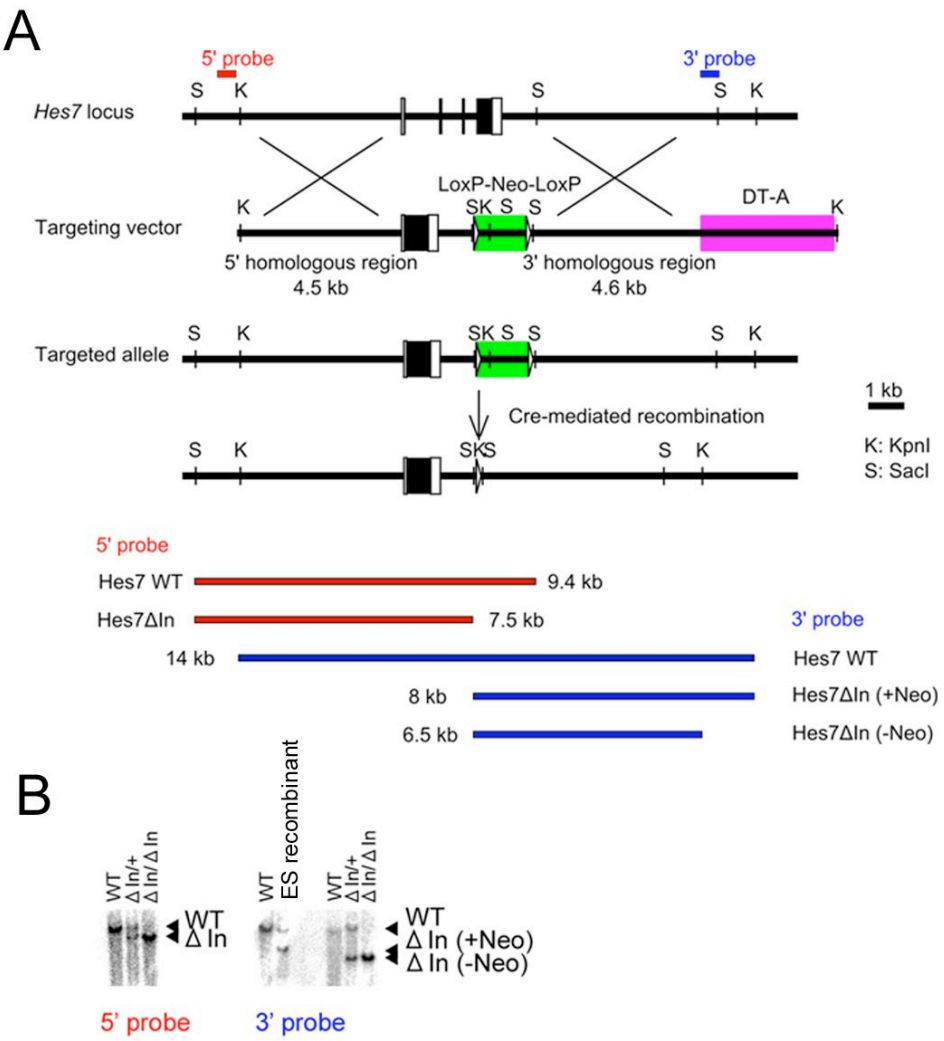

Supplemental Figure S5. Deletion of all introns from the *Hes7* locus. (*A*) Strategy for generation of the intron-less *Hes7* allele. Closed and open squares indicate coding and non-coding regions of *Hes7*, respectively. A neomycin resistant gene cassette (Neo^r) flanked by LoxP sites was inserted into the SacI site in the 3'-downstream region in the targeting vector. The diphtheria toxin A (DT-A) gene was used as a negative selection marker. The targeting vector was introduced into mouse ES cells, and after obtaining homologous recombinant ES cells, Neo^r was removed by Cre. Bands with sizes detected by 5'- and 3'-probes are indicated at the bottom. (*B*) Southern blotting analysis of genomic DNA extracted from embryos or ES cells. DNA was digested with SacI for the 5' probe and KpnI for the 3' probe.

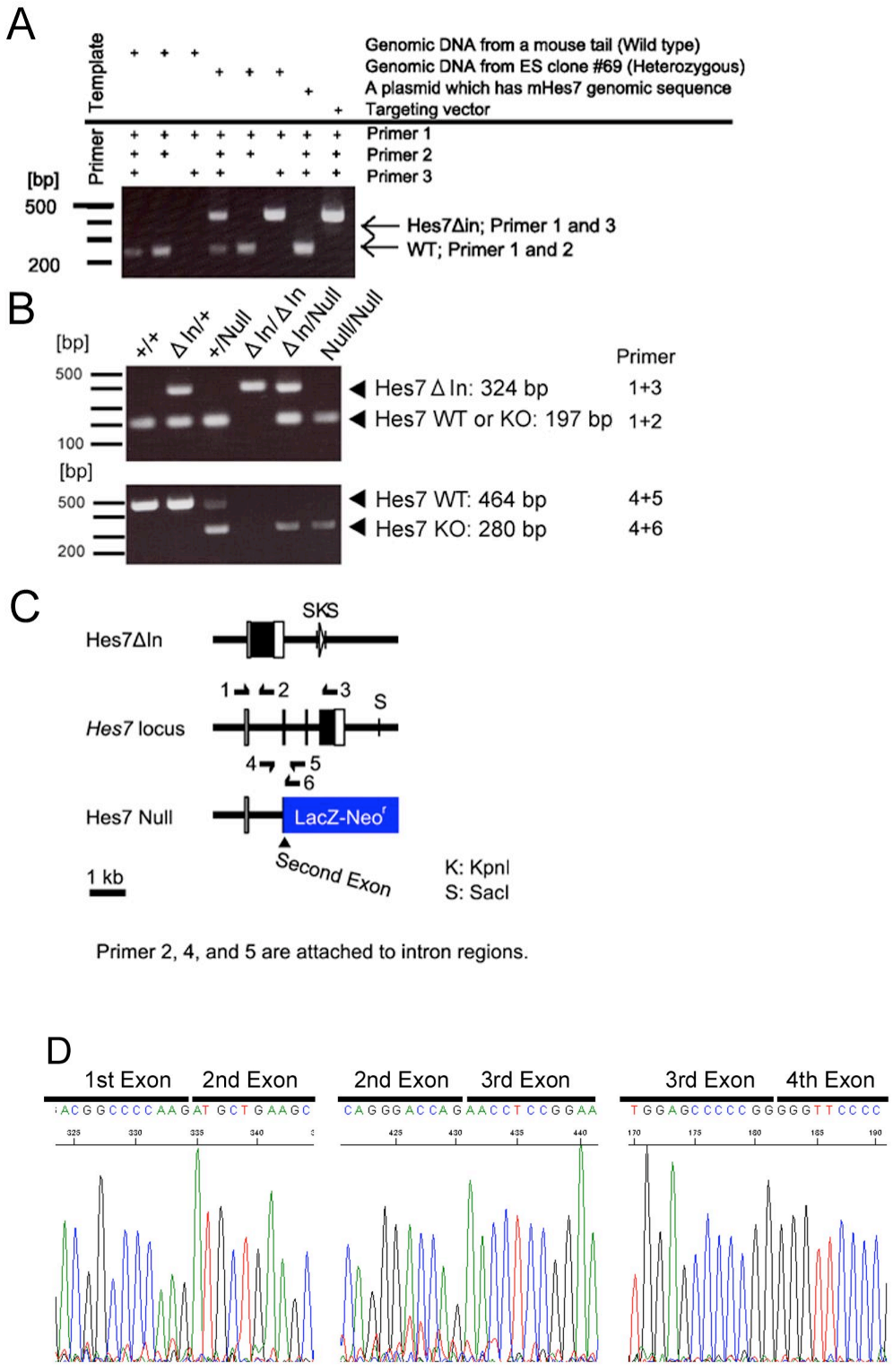

Supplemental Figure S6. Genotyping of *Hes7*-mutant mice and verification of the intron-less mutation. (*A*,*B*) PCR analysis for genotyping. Genomic DNA from the ES cells (*A*) and mouse tails (*B*) was used as a template. (*C*) The positions of primers are

indicated by arrows. (*D*) Verification of the absence of the introns. Genomic DNA of the intron-less mice was isolated and sequenced by PCR. In these mice, all introns were removed from the *Hes7* locus.

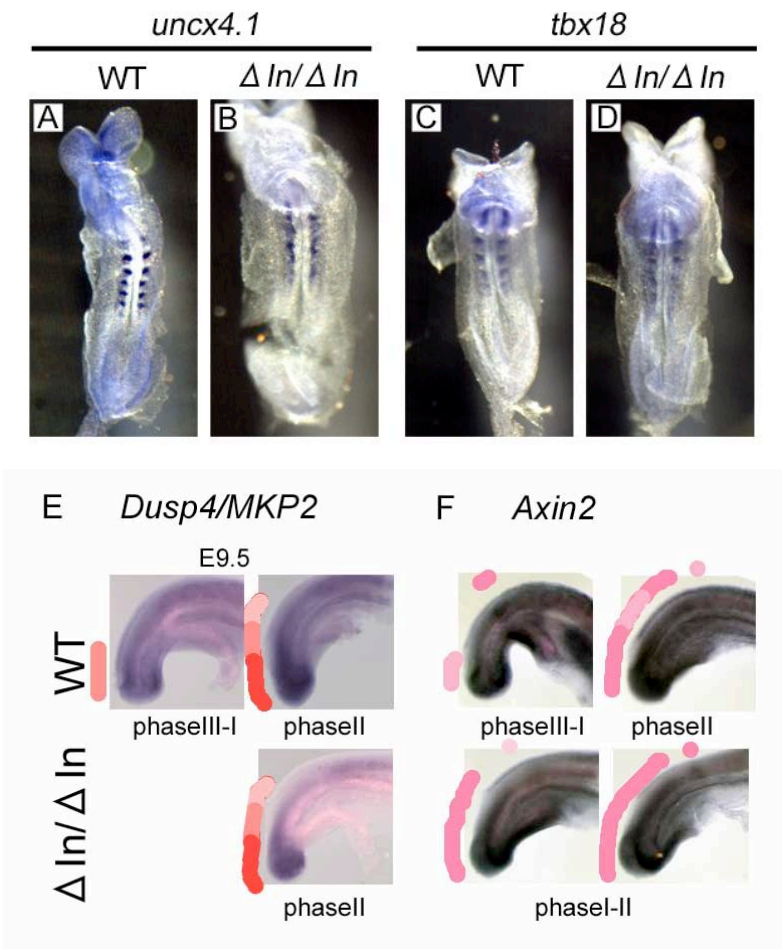

Supplemental Figure S7. Patterning defects in *Hes7* intron-less mice. (*A-D*) *Uncx4.1* (*A,B*) and *Tbx18* (*C,D*) expression in E8.5 wild-type (*A,C*) and *Hes7* intron-less (*B,D*) embryos were examined by in situ hybridization. *Uncx4.1* and *Tbx18* expression was not properly segmented in *Hes7* intron-less mice. Anterior is to the top in all panels. (*E*) *Dusp4/MKP2* and *Axin2* expression. *Dusp4/MKP2* expression oscillates in wild-type embryos at E9.5. n = 4/9 (phase III-I), 5/9 (phase II). (lower left panels) By contrast, *Hes7* intron-less mice lose the oscillation of *Dusp4/MKP2* expression. n = 4. (*F*) *Axin2* expression was dynamic in wild-type embryos at E9.5. n = 7/9 (phase III-I), n = 2/9 (phase II). (lower right panels) *Axin2* expression was still variable but less dynamic in *Hes7* intron-less embryos. n = 2/7 (phase I), n = 5/7 (phase II).

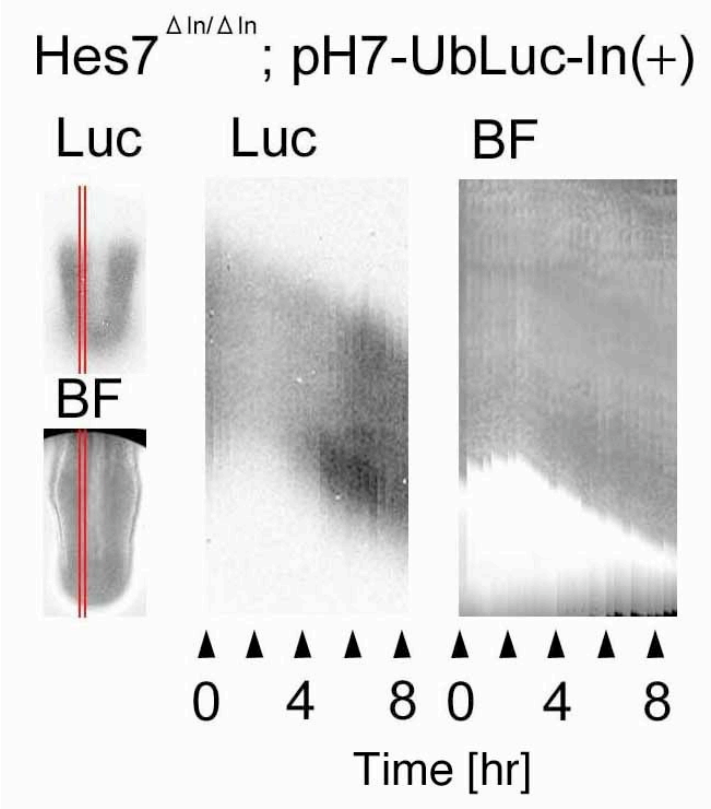

Supplemental Figure S8. Reporter expression in *Hes7* intron-less mice. pH7-UbLuc-In(+) reporter was introduced into *Hes7* intron-less mice. Real-time imaging of *Hes7* promoter activity in the PSM explant culture was performed (Luc), and spatiotemporal profiles of the reporter expression were made. Oscillatory reporter expression was not detectable, although some difference in amplitude was observed. Clear segmentation was not observed in a bright field (BF).

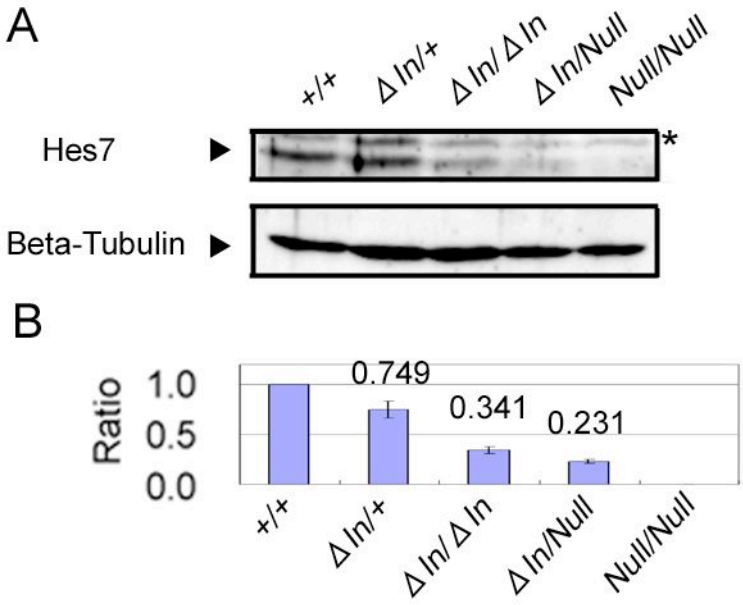

Supplemental Figure S9. Western blot analysis of Hes7 expression in the PSM. (*A*) Proteins were extracted from the posterior parts of embryos, and the average expression levels of Hes7 protein were analyzed by western blot. The asterisk indicates a non-specific band. (*B*) Relative average levels of Hes7 protein expression. The average of three independent samples with a standard error was determined for each genotype. Each value was normalized with that of β–tubulin. About 34% of the wild-type levels of Hes7 protein was expressed in *Hes7* intron-less mice (ΔIn/ΔIn).

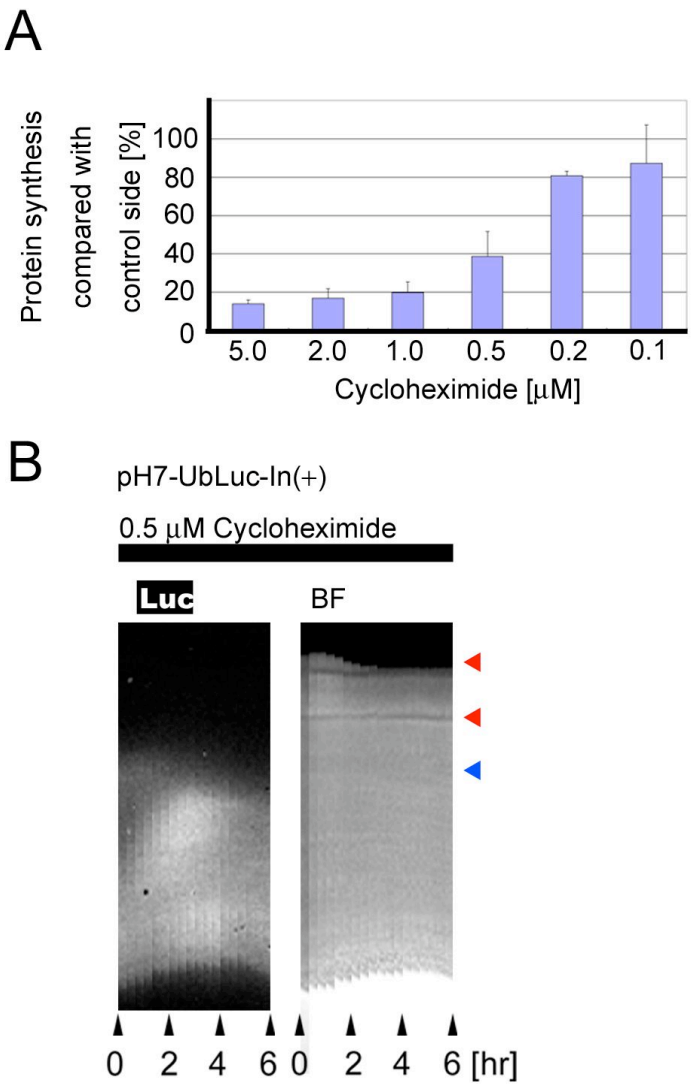

Supplemental Figure S10. *Hes7* oscillations persist when protein synthesis is inhibited. (*A*) The rates of protein synthesis inhibition by cycloheximide. Bisected posterior parts of embryos were cultured with or without cycloheximide. Protein synthesis rates were calculated by comparing ^{35}S incorporation rates between the two samples. The average of three independent samples with a standard error was determined. (*B*) Real-time imaging of *Hes7* promoter activity in the PSM cultured in the presence of 0.5μM cycloheximide. The left panel shows spatiotemporal promoter activity of pH7-UbLuc-In(+) embryos and the right panel shows bright field images. While the bioluminescence signal was weak, it still oscillated (left). Red arrowheads show boundaries of somites. The latest boundary shown in blue arrowhead was difficult to see in this panel because inhibition of protein synthesis perturbed somite boundary formation.

Supplemental Movie 1. Time-lapse images of the PSM of a pH7-UbLuc-In(−) embryo at E10.5. Images were taken by 20 min exposure and binning of pixels 4 x 4 over a period of 10 hours. Oscillations were propagated from the posterior to the anterior PSM.

Supplemental Movie 2. Time-lapse images of the PSM of a pH7-UbLuc-In(+) embryo at E10.5. Images were taken by 20 min exposure and binning of pixels 4 x 4 over a period of 10 hours. Oscillations were propagated from the posterior to the anterior PSM.

References

1. Hirata H, Bessho Y, Kokubu H, Masamizu Y, Yamada S, Lewis J, Kageyama R (2004) Instability of Hes7 protein is crucial for the somite segmentation clock. *Nat Genet* **36:** 750-754.
2. Fall CP, Marland ES, Wagner JM, Tyson JJ (2000) *Computational Cell Biology* Springer.
3. Rateitschak K, Wolkenhauer O (2007) Intracellular delay limits cyclic changes in gene expression. *Math Biosci* **205:** 163-179.
4. Bessho Y, Hirata H, Masamizu Y, Kageyama R (2003) Periodic repression by the bHLH factor Hes7 is an essential mechanism for the somite segmentation clock. *Genes Dev* **17:** 1451-1456.